



Article

Influence of the Incorporation of Nd in ZnO Films Grown by the HFCVD Technique to Enhance Photoluminescence Due to Defects

Marcos Palacios Bonilla ^{1,*}, Godofredo García Salgado ^{1,*}, Antonio Coyopol Solís ¹, Román Romano Trujillo ¹, Fabiola Gabriela Nieto Caballero ² , Enrique Rosendo Andrés ¹ , Crisóforo Morales Ruiz ¹, Justo Miguel Gracia Jiménez ³ and Reina Galeazzi Isasmendi ¹

- ¹ Centro de Investigación en Dispositivos Semiconductores, Benemérita Universidad Autónoma de Puebla, Ed. IC5, Av. San Claudio y Blvd. 18 Sur, Col. San Manuel, Puebla 72570, Mexico; antonio.coyopol@correo.buap.mx (A.C.S.); roman.romano@correo.buap.mx (R.R.T.); enrique.rosendo@correo.buap.mx (E.R.A.); crisoforo.morales@correo.buap.mx (C.M.R.); reina.galeazzi@correo.buap.mx (R.G.I.)
- ² Facultad de Ciencias Químicas, Benemérita Universidad Autónoma de Puebla, Ed. FCQ4, Av. San Claudio y Blvd. 18 Sur, Col. San Manuel, Puebla 72570, Mexico; fabiola.nieto@correo.buap.mx
- ³ Instituto de Física, Benemérita Universidad Autónoma de Puebla, Av. San Claudio y Blvd. 18 Sur, Col. San Manuel, Puebla 72570, Mexico; gracia@ifuap.buap.mx
- * Correspondence: marcos.palaciosbonilla@alumno.buap.mx (M.P.B.); godofredo.garcia@correo.buap.mx (G.G.S.)



Citation: Palacios Bonilla, M.; García Salgado, G.; Coyopol Solís, A.; Romano Trujillo, R.; Nieto Caballero, F.G.; Rosendo Andrés, E.; Morales Ruiz, C.; Gracia Jiménez, J.M.; Galeazzi Isasmendi, R. Influence of the Incorporation of Nd in ZnO Films Grown by the HFCVD Technique to Enhance Photoluminescence Due to Defects. *Crystals* **2024**, *14*, 491. <https://doi.org/10.3390/cryst14060491>

Academic Editors: Miłosz Grodzicki, Damian Wojcieszak and Michał Mazur

Received: 25 April 2024

Revised: 14 May 2024

Accepted: 16 May 2024

Published: 23 May 2024



Copyright: © 2024 by the authors. Licensee MDPI, Basel, Switzerland. This article is an open access article distributed under the terms and conditions of the Creative Commons Attribution (CC BY) license (<https://creativecommons.org/licenses/by/4.0/>).

Abstract: In this work, optical–structural and morphological behavior when Nd is incorporated into ZnO is studied. ZnO and Nd-doped ZnO (ZnO-Nd) films were deposited at 900 °C on Silicon n-type substrates (100) by using the Hot Filament Chemical Vapor Deposition (HFCVD) technique. For this, pellets were made by from powders of ZnO(s) and a mixture of ZnO(s):Nd(OH)₃(s). The weight percent of the mixture ZnO:Nd(OH)₃ in the pellet is 1:3. The gaseous precursor generation was carried out by chemical decomposition of the pellets using atomic hydrogen which was produced by a tungsten filament at 2000 °C. For the ZnO film, diffraction planes (100), (002), (101), (102), (110), and (103) were found by XRD. For the ZnO-Nd film, its planes are displaced, indicating the incorporation of Nd into the ZnO. EDS was used to confirm the Nd in the ZnO-Nd film with an atomic concentration (at%) of Nd = 10.79. An improvement in photoluminescence is observed for the ZnO-Nd film; this improvement is attributed to an increase in oxygen vacancies due to the presence of Nd. The important thing about this study is that by the HFCVD method, ZnO-Nd films can be obtained easily and with very short times; in addition, some oxide compounds can be obtained individually as initial precursors, which reduces the cost compared to other techniques. Something interesting is that the incorporation of Nd into ZnO by this method has not yet been studied, and depending on the method used, the PL of ZnO with Nd can increase or decrease, and by the HFCVD method the PL of the ZnO film, when Nd is incorporated, increases more than 15 times compared to the ZnO film.

Keywords: HFCVD; silicon; ZnO-Nd; sea urchin

1. Introduction

ZnO presents n-type electrical conductivity and has a wide direct bandgap of ~3.37 eV at room temperature [1,2]. In addition, it presents interesting properties such as: high chemical and thermal stability; good optical and electrical properties; high transparency in the Vis/near-IR spectral region [3]; and a large exciton binding energy of 60 mV [2,4–6]. Such properties have allowed ZnO to be used in optoelectronic device applications such as: gas sensors [7], solar cells [8], ultraviolet (UV) detectors [9], light-emitting diodes, and lasers [10]. On the other hand, ZnO presents a better optical response in PL intensity and a

low band gap when it is doped and forms compounds with different chemical elements, for example Nd [11], Ni [12], and Ta [13]. Doping ZnO with metal atoms such as Nd introduces new properties in ZnO that are useful in different areas such as photocatalysis and optoelectronics [14,15]. Nd-doped ZnO films enhance PL intensity at deep level emissions (~511 nm) [11]. Some methods such as spray pyrolysis [14], pulsed electron beam [16], and sol-gel [17], have been used to obtain Nd-doped ZnO films. However, using the HFCVD technique for this process has not been explored. The HFCVD technique allows the obtention of high deposit rates, so long times for film growth are not necessary. In addition, solid sources have been used for the formation of gaseous precursors for the deposit of materials such as: ZnO [18], ZnO-Ni [12], and ZnO-Ta [13]. Therefore, the study of ZnO with the incorporation of Nd from a solid pellet based on a mixture of ZnO(s):Nd(OH)₃(s), attacked with atomic hydrogen (H[°]), is feasible. The atomic hydrogen is produced by using a tungsten filament at 2000 °C, etching the solid source (pellet) to obtain chemical precursors that diffuse and deposit on a Si substrate [13,19]. The HFCVD process has been reported in other works [18,20]. Using the HFCVD technique, sphere-shaped structures of ZnO can be grown, which have a large surface–volume ratio which is important for devices such as drug delivery devices [21] and gas sensors [18], and in solar energy conversion and field emission [18,22]. Thus, the objective of this work is to study the structural, morphological, and optical properties of ZnO and compare them with ZnO-Nd films on silicon substrates.

2. Experimental Details

2.1. Pellets Preparation

A ZnO(s):Nd(OH)₃(s) pellet (0.4 g) was prepared by compressing ZnO(s) powder (Sigma-Aldrich CAS-No:1314-13-2, Estado de México, México) combined with Nd(OH)₃(s) powder (Sigma-Aldrich CAS-No:16469-17-3). The weight percent of the mixture ZnO(s):Nd(OH)₃(s) in the pellet was 1:3. The reason that the pellet was in that proportion is because the amount of Nd that can be released from the ZnO:Nd(OH)₃ pellet in the film growth process is minimal (less than 1% in weight percentage). In addition, the 1:3 ratio was prepared because other samples were made and it was observed that the PL intensity increases as the Nd in the ZnO increases, and this sample is very interesting and high in PL intensity. The quantities used in each pellet of this work are shown in Table 1.

Table 1. Experimental conditions used for ZnO and ZnO-Nd films.

Film	Pellet	Proportion in Weight Percentage ZnO:Nd(OH) ₃	ZnO Weight (g)	Nd(OH) ₃ Weight (g)	Substrate Temperature (°C)	Process Time (min.)
ZnO	ZnO	1:0	0.4	0	900	3
ZnO-Nd	ZnO:Nd(OH) ₃	1:3	0.1	0.3	900	3

2.2. Growth Process of ZnO and ZnO-Nd Films

Silicon n-types with orientation (100) and resistivity 1–20 Ω·cm were used as substrates. Firstly, Si-substrates were cleaned following a process in an ultrasonic bath for 10 min in each chemical solution, including: xylene, acetone, and methanol. Additionally, Si substrates were immersed for 1 min in HF (10%) to remove native oxide. For the film growth process, H₂ flow (50 sccm) was incorporated in reaction chamber (Figure 1a); afterwards, atomic hydrogen (H[°]) was produced by a tungsten filament at 2000 °C., although the growth temperature used for deposits was 900 °C for 3 min. The generation of gaseous precursors occurred through the reaction of a solid source (pellet based on a mixture of ZnO(s) and Nd(OH)₃(s)) with atomic hydrogen (Figure 1b).

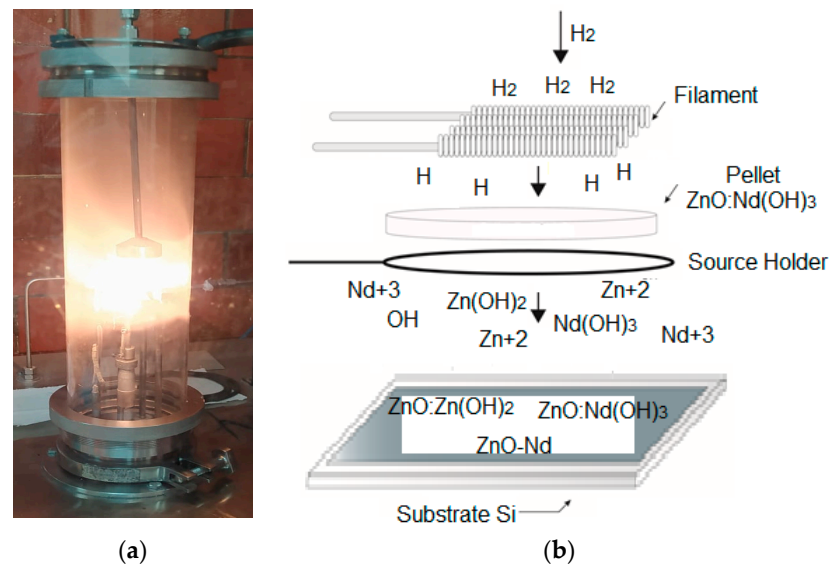
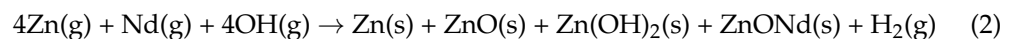
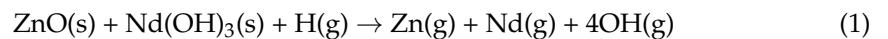


Figure 1. (a) HFCVD reactor and (b) internal configuration of HFCVD reactor.

Regarding the reaction for ZnO films grown using the HFCVD technique, it has already been reported in other works [23]. On the other hand, for the ZnO-Nd film grown in this work, the substrate chemical reactions are presented as follows:



Finally, XRD, SEM, EDS, and PL measurements were performed. The structural characterization was carried out with an X-ray diffractor (BRUKER D8 with Cu K α radiation ($\lambda = 1.541 \text{ \AA}$), Billerica, MA, USA). The surface morphology and elements of the samples were characterized by using a Jeol JSM-7800F (JEOL Ltd., Tokyo, Japan) field emission scanning electron microscope equipped with an Oxford Instrument X-Max spectrometer for elemental analysis (JEOL Ltd., Tokyo, Japan). Photoluminescence measurements were performed at room temperature with a Horiba Jobin Yvon NanoLog FR3 UV-Vis-NIR fluorescence spectrometer (Horiba Ltd., Kyoto, Japan).

3. Results and Discussion

3.1. Structural Characterization by X-ray Diffraction (XRD) Analysis

ZnO and ZnO-Nd films were analyzed using XRD. Figure 2 shows the pattern of XRD for the samples measured from 25° to 65° in the 2θ mode. For the ZnO film in the (a) pattern, three Zn planes (100), (101), and (102) located at 39.16° , 43.38° and 54.42° are observed, which match with the Zn hexagonal structure of the pdf card 004-0831. It is observed that the planes (100), (002), (101), (102), (110), and (103) of ZnO which are located at 31.98° , 34.6° , 36.44° , 47.74° , 56.78° , and 63.08° match according to the wurtzite ZnO structure of the pdf card 075-0576. In pattern (b), for the ZnO-Nd film the same ZnO film planes are observed. Furthermore, it can be observed that the ZnO-Nd film planes shift slightly to the left compared to the ZnO film planes, and it is suggested that this slight shift is due to the change in lattice parameters; however, the wurtzite structure of the crystal remains unchanged [24]. So, for this reason it is suggested that Nd is incorporated into the ZnO matrix. This shift is due to the difference in the ionic radii of Zn^{+2} and Nd^{+3} . Since the ionic radius of Nd^{+3} (0.983 \AA) is larger than that of Zn^{+2} (0.74 \AA), an expansive stress is created in the lattice; therefore, it is suggested that there is an expansion in the ZnO lattice resulting in the displacement of the ZnO-Nd planes and it is suggested that this expansion in the crystal lattice confirms that Nd is introduced substitutionally into the ZnO lattice [15,24].

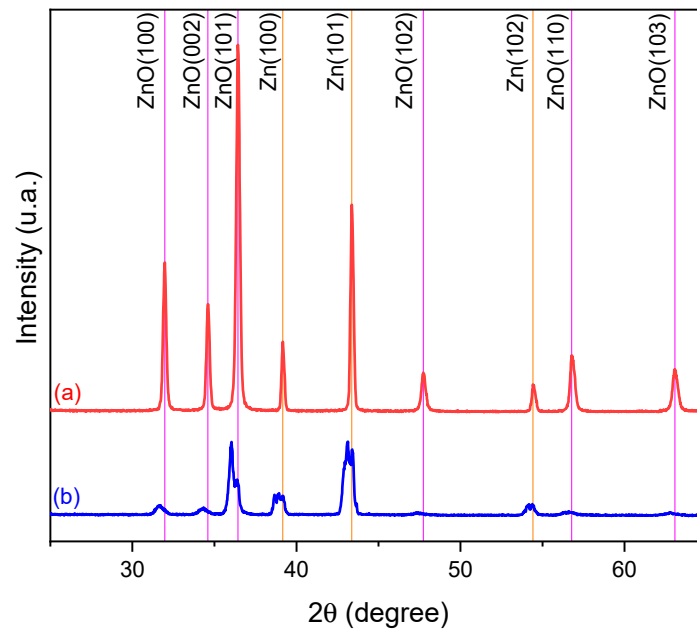


Figure 2. X-ray diffraction patterns for (a) ZnO and (b) ZnO-Nd films.

Figure 3 analyzes Figure 2 better: the planes of ZnO, Zn, Zn(OH)₂, and Nd(OH)₃ are shown with different symbols. In the ZnO film (Figure 3a), the ZnO and Zn planes are observed, so the core-shell structures are observed, where the metallic Zn is the core and the ZnO is the shell [12,13]. In addition, the Zn(OH)₂ planes [25] are observed because in the film growth process some Zn⁺² joins with the OH that is being transported, forming Zn(OH)₂; then, some Zn(OH) is also deposited on the surface of the film, remaining in the form of ZnO:Zn(OH)₂ composites. In the ZnO-Nd film (Figure 3b), the same planes of the ZnO film are observed; however, some Nd(OH)₃ planes [26] also appear. This is because in the film growth process some Nd⁺³ atoms join with the OH that is being transported, forming Nd(OH)₃, and for this reason some Nd(OH)₃ is also deposited on the surface of the film, remaining in the form of ZnO:Nd(OH)₃ composites. In addition, the Zn(OH)₂ planes [25] are observed, so there are also some ZnO:Zn(OH)₂ composites on the surface of the film.

To calculate the lattice parameters, Equation (3) is used:

$$\frac{1}{d_{(hkl)}^2} = \frac{4}{3a^2} (h^2 + k^2 + hk) + \frac{1}{c^2} \quad (3)$$

In this way, the interplanar spacing $d_{(hkl)}$ can be obtained from the relation $\frac{1}{d_{hkl}} = \frac{2\sin\theta}{\lambda}$, where h,k,l are the miller indices of the respective plane, and a and c are the lattice parameters which are calculated with the (100), and (002) planes at 31.98° and 34.6° [12]. Table 2 shows the lattice parameters for the (002) plane of the different films obtained in this work.

Table 2. Lattice parameters of ZnO and ZnO-Nd films of plane (002).

Sample	a (Å)	c (Å)	c/a
ZnO	3.2289	5.1806	1.6044
ZnO-Nd	3.2547	5.2187	1.6034

It can be seen in Table 2 that the parameter “c” increases and the parameter “a” increases, and so for these reasons, it is suggested that Nd⁺³ is incorporated into the ZnO lattice in a substitutional manner, and it is proposed that Nd⁺³ ions replace Zn⁺² ions, thus obtaining Nd-doped ZnO [24].

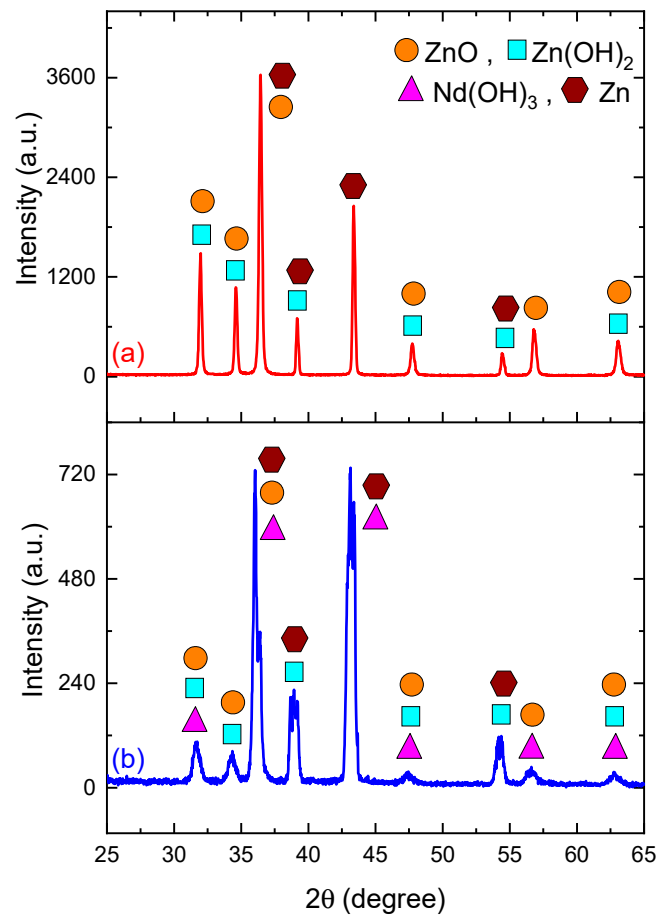
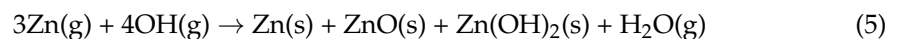
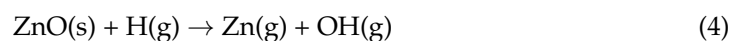


Figure 3. A better analysis of Figure 2 is shown for the XRD patterns of (a) ZnO and (b) ZnO-Nd films.

3.2. Scanning Electron Microscope (SEM)

SEM measurements were made to observe the morphology of the ZnO and ZnO-Nd films. Figure 4a,b shows the ZnO film and Figure 4c–f shows the ZnO-Nd film at different zoom levels.

SEM images in Figure 4a,b, for a ZnO film, show sphere-type structures on the surface of the film. It is suggested that the growth process of sphere-type structures occurs when molecular hydrogen enters into the reactor through the filament at 2000 °C and decomposes in atomic hydrogen, which attacks the ZnO(s) pellet, forming the precursors Zn(g) and OH(g) as proposed in [13,27], starting with the following chemical reactions:



Molecular hydrogen decomposes into atomic hydrogen due to the temperature of the filament. The atomic H releases Zn and O atoms from the ZnO pellet, according to reaction 4. In reaction 5, core–shell (Zn/ZnO) structures are formed on the silicon substrate; this is deduced from the XRD planes of Zn and ZnO [12,13]. Figure 4b shows the surface of an individual ZnO sphere (Figure 4a) with a zoom of $\times 1000$. Figure 4c–f show the ZnO-Nd film. The formation process of ZnO-Nd spheres is similar to that of ZnO spheres; the difference is that ZnONd structures are formed in the former. It can be observed the sphere-like structure that it has on its surface is like wires; this is suggested to be because the Nd atoms act as a catalyst and nucleate, resulting in a sea urchin-like structure [28]. Furthermore, it can be observed that when Nd is incorporated, there is a decrease in the size of the spheres. It is observed that the spheres on the ZnO-Nd film have a smaller size than in the ZnO film and it is suggested that the decrease in the size of the ZnO-Nd spheres

is due to the incorporation of Nd. That is to say, it is due to the nucleation mechanism in the growth process; because the ionic radius of Nd^{+3} is greater than that of Zn^{+2} , it has a lower nucleation rate than in the ZnO film which results in a smaller sphere size [29]. From Figure 4b,d ($\times 1000$), it is estimated that the ZnO spheres are larger, since in the ZnO sphere (Figure 4b) only part of the surface of an individual ZnO sphere can be observed, and Figure 4d shows complete ZnO-Nd spheres because they are smaller in size. Figure 5 shows the distribution of the different chemical elements for the ZnO-Nd film. Figure 6 shows each chemical element individually. The film appears relatively homogeneous; however, it can be seen that there is an agglomeration of many Nd atoms (as also seen in Figure 4f), which suggests that there is a ZnO:Nd(OH)_3 composite because in XRD the Nd(OH)_3 planes for the ZnO-Nd film are observed.

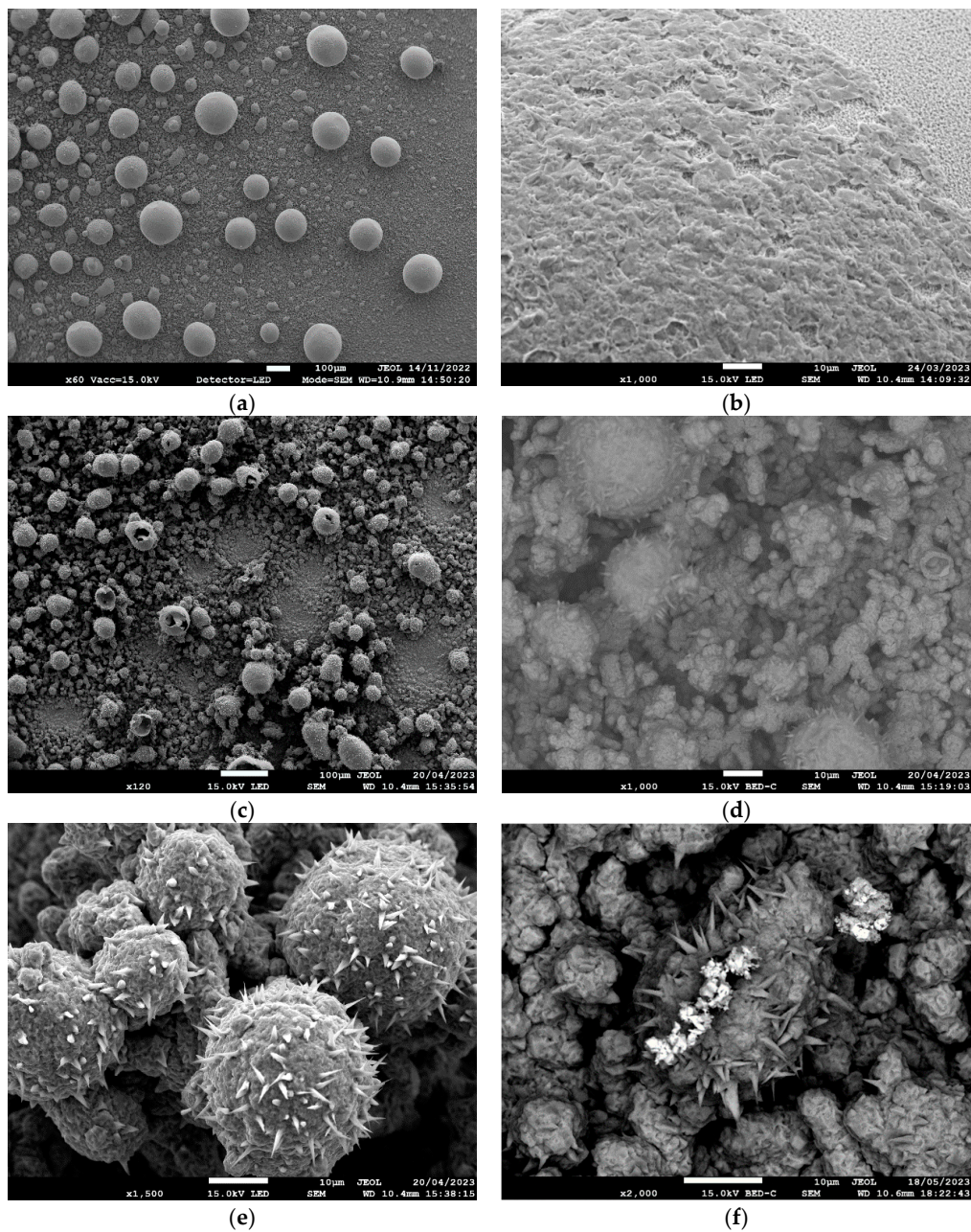


Figure 4. SEM for (a,b) ZnO and (c–f) ZnO-Nd films at different zoom levels.

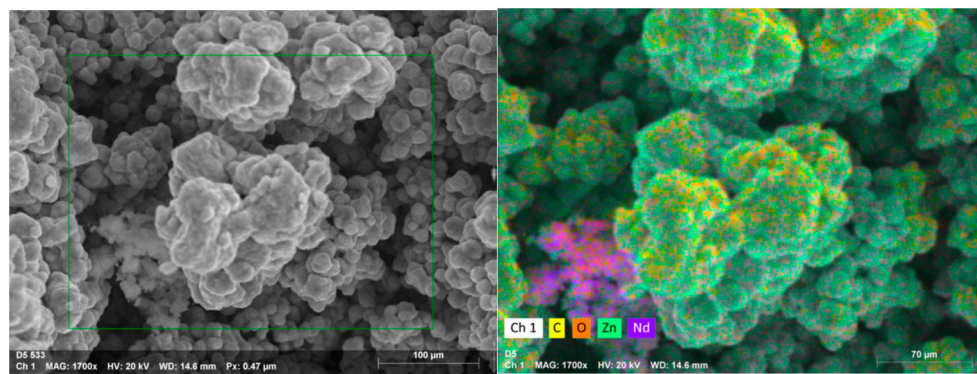


Figure 5. Color mapping of the different chemical elements of the ZnO-Nd film.

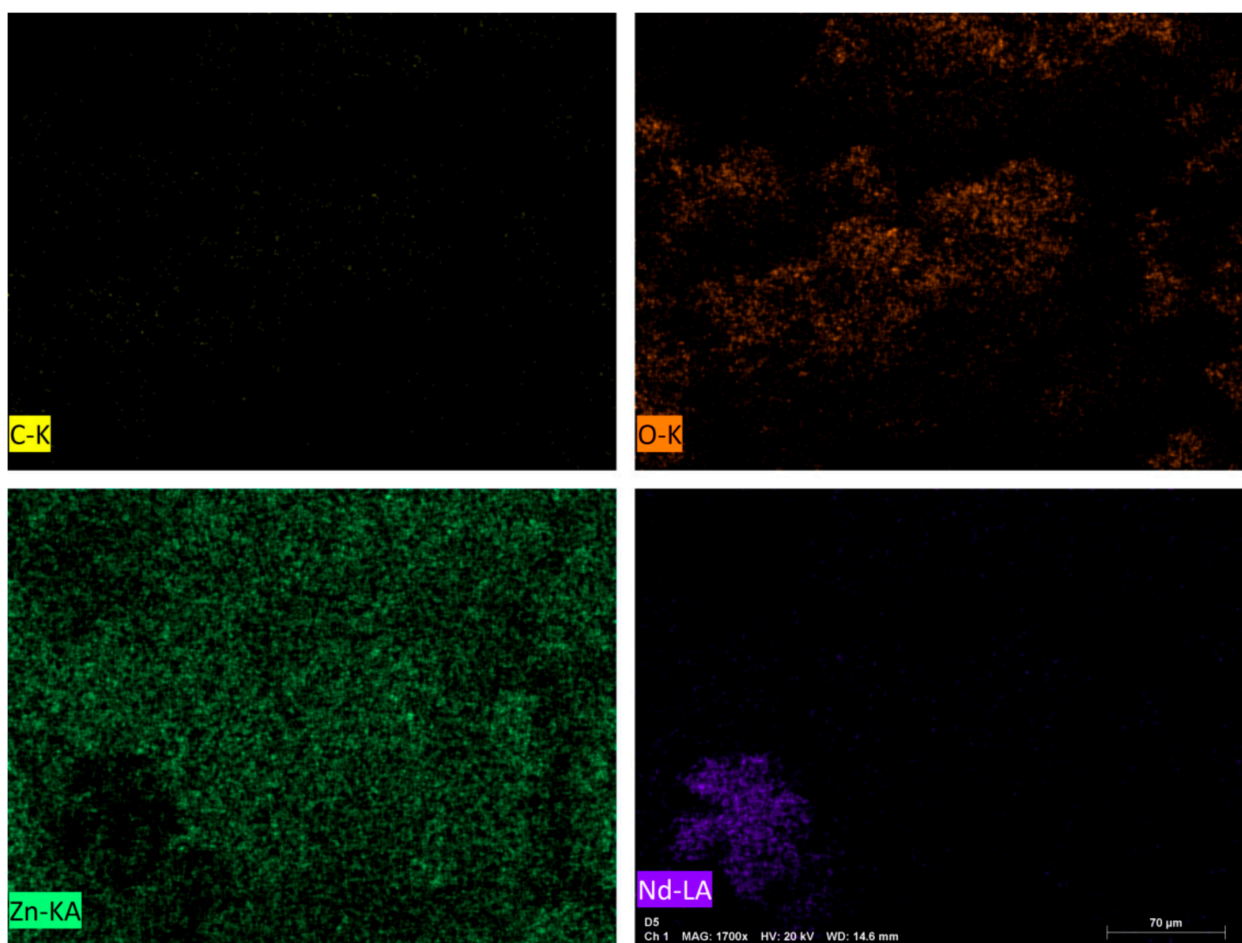


Figure 6. Chemical elements individually for the ZnO-Nd film.

3.3. Energy Dispersive X-ray (EDS) Analysis

Figure 7a shows the EDS analysis for the ZnO film. In the EDS of the ZnO film, it is observed that the film presents the chemical elements of Zn and O. For this reason, it is suggested that when the H impacts the ZnO pellet, it decomposes it into Zn and O atoms that begin to be transported into the reactor. Subsequently, the Zn, due to its boiling point (907 °C), adheres to the substrate (900 °C) due to the temperature difference and remains as a nucleation site, but since the O atoms are also being transported, they begin to bind to the Zn and, thus, the ZnO film is obtained [13]. The carbon peak corresponds to the piece of paper used in the SEM measurement. Figure 7b shows the EDS of the ZnO-Nd film, where the presence of Nd is confirmed. It is observed that the film presents the chemical

elements of Zn, O, and Nd. In the ZnO-Nd film, something very similar happens: the H impacts the ZnO:Nd(OH)₃ pellet and decomposes it into Zn, O, and Nd atoms that begin to be transported inside the reactor; in this way, ZnO is formed as described above, but since Nd atoms are also being transported here, they begin to bind to the O of ZnO and, thus, the ZnO-Nd film is obtained [13]. Table 3 shows the different compositions of the ZnO and ZnO-Nd films.

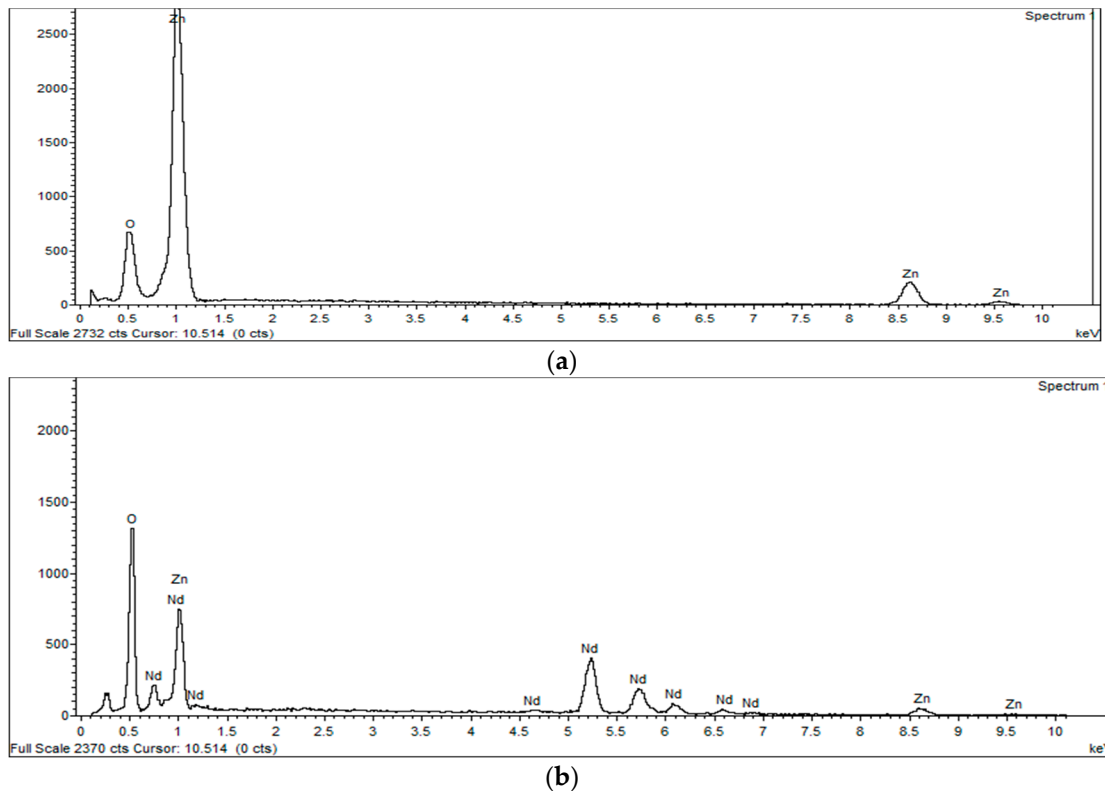


Figure 7. (a) EDS for ZnO film. (b) EDS for ZnO-Nd film.

Table 3. Average atomic percentage of elemental composition of ZnO and ZnO-Nd films.

Sample	Zn (%)	O (%)	Nd (%)
ZnO	69.36	30.64	0
ZnO-Nd	43.99	45.22	10.79

It can be seen that the ZnO film has an atomic percentage of approximately Zn = 69.36%, which suggests that it is a film rich in zinc. It can be observed in the ZnO-Nd film (Figure 4f) that there is approximately an atomic percentage of Nd = 10.79%; therefore, the presence of Nd is confirmed. For Figure 4e, there is an average atomic percentage of Nd = 1.25%, Zn = 63.64%, and O = 35.11% so it is suggested that there is doping; however, in Figure 4f it can be seen that an agglomerate of Nd remained on the surface of the film with Nd = 10.79% (Table 3), so it is suggested that it is also a ZnO:Nd(OH)₃ composite, and this can be seen better in Figure 6.

3.4. Photoluminescence Analysis (PL)

Figure 8 shows the PL spectra of the ZnO and ZnO-Nd films at room temperature measured from 350 to 750 nm, with the purpose of studying the behavior of Nd in the ZnO.

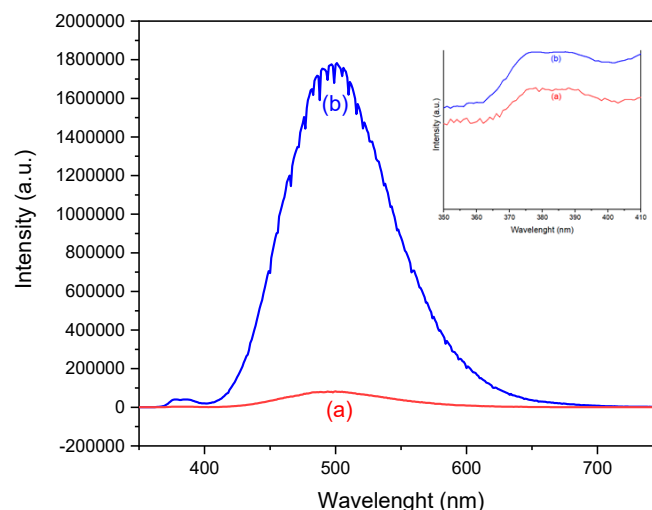


Figure 8. Photoluminescence spectra of (a) ZnO and (b) ZnO-Nd films. A PL graph is also presented with a zoom in the NBE region of ~ 380 nm.

For the ZnO film, a band ~ 380 nm named as near-band-edge emission NBE is observed, and this is due to the band-to-band transition [13]; the band ~ 502 nm, called the deep level emission which is abbreviated to DLE, is due to the transitions through deep centers with energy levels in the forbidden gap of the hydroxyl group, and is also due to different defects in the lattice, such as oxygen or zinc interstitials, oxygen or zinc vacancies, or external impurities due to the substitution of atoms [13,29,30]. For the ZnO-Nd film, an increase in the intensity of the DLE band is observed. It is suggested that this is because when Nd is incorporated into the ZnO, more defect centers such as oxygen vacancies are created and for this reason a PL increase occurs [31]. In addition, due to the distortion of the lattice as mentioned in XRD, and other defects, it is suggested that the energy gaps are split and for this reason a greater wavelength range is covered in the PL spectrum [32]. From SEM, it can be observed that there is a decrease in the size of the spheres, and because it is reported in the literature that, when there is a decrease in particle size, more oxygen vacancies are created, it is suggested that for this reason the PL also increases [30]. Furthermore, in Figure 8 for the ZnO and ZnO-Nd films, in the NBE band region, two different bands are observed that correspond to ZnO (~ 380 nm) and Zn(OH)_2 (~ 387 nm) [33]. The two bands, NBE and DLE, of Zn(OH)_2 are similar to the two bands (NBE and DLE) of ZnO, only the intensity of the PL varies a little [33]. Based on the PL results and because the Zn(OH)_2 planes are observed in XRD, it is suggested that there are also some $\text{ZnO}:\text{Zn(OH)}_2$ composites on the surface of the ZnO and ZnO-Nd films.

4. Conclusions

The objective of this research is to observe how Nd(OH)_3 behaves when reacting with ZnO using the HFCVD method, since ZnO-Nd formed by this technique has not yet been explored; in addition, with growth by HFCVD, ZnO and ZnO-Nd films are obtained relatively easily and with short times. Therefore, the structural, morphological, and optical properties of ZnO and ZnO-Nd films on silicon substrates are studied. From XRD studies, it is observed that the ZnO planes match with the hexagonal wurtzite structure of ZnO. It is also observed in the diffractogram that there is a displacement of the planes of the ZnO-Nd film, which is due to the fact that the Nd is incorporated into the ZnO, thus achieving doping. Furthermore, the planes of Zn, ZnO, Zn(OH)_3 , and Nd(OH)_3 are observed individually, so the presence of a $\text{ZnO}:\text{Nd(OH)}_3$ composite is also noted. From the SEM results, the different morphology observed in the sphere-like structures of the ZnO-Nd film is due to the fact that the Nd atoms act as a catalyst and nucleate, resulting in a structure similar to that of a sea urchin. It is also observed that the sphere-like structures in the ZnO-Nd film have a smaller size than in the ZnO film; this is due to the incorporation of Nd in the ZnO. In addition,

from the different morphology and decrease in size of the ZnO-Nd spheres, it is deduced that the Nd is doping the ZnO; however, as some agglomerations of Nd(OH)₃ are also observed on the surface of the film, it is deduced that it is also a ZnO:Nd(OH)₃ composite. EDS analysis confirms the presence of Nd. Furthermore, in the ZnO-Nd sphere there is a low average atomic percentage of Nd = 1.25%, so it can be deduced that there is doping; however, in the Nd(OH)₃ agglomeration, there is a higher average atomic percentage of Nd = 10.79%, and so it follows that there is also a ZnO:Nd(OH)₃ composite. From the PL measurement, when Nd is incorporated into ZnO as a dopant, it causes an increase in O vacancies, thus achieving an increase in the intensity of photoluminescence. For these reasons, it is deduced that composites and doping coexist and are present in the ZnO-Nd film.

Author Contributions: M.P.B. and G.G.S. wrote, conceived, and designed the experiments; A.C.S., J.M.G.J. and E.R.A. provided resources and systems; R.R.T., F.G.N.C., C.M.R. and R.G.I. provided support in review and editing this work. All authors have read and agreed to the published version of the manuscript.

Funding: This research received no external funding.

Data Availability Statement: The original contributions presented in the study are included in the article; further inquiries can be directed to the corresponding author.

Acknowledgments: The authors thank CONAHCYT and ICUAP for the use of the facilities.

Conflicts of Interest: The authors declare no conflicts of interest. The funders had no role in the design of the study; in the collection, analyses, or interpretation of data; in the writing of the manuscript; or in the decision to publish the results.

References

1. Sauvik, R.; Ahmaruzzaman, M. ZnO nanostructured materials and their potential applications: Progress, challenges and perspectives. *Nanoscale Adv.* **2022**, *4*, 1868–1925. [[CrossRef](#)] [[PubMed](#)]
2. Yıldırım, A.K.; Altıokka, B. Effect of Potential on Structural, Morphological and Optical Properties of ZnO Thin Films Obtained by Electrodeposition. *J. Mater. Sci. Eng.* **2015**, *B5*, 107–112. [[CrossRef](#)]
3. Chebil, W.; Fouzri, A.; Azeza, B.; Sakly, N.; Mghaieth, R.; Lusso, A.; Sallet, V. Comparison of ZnO thin films on different substrates obtained by sol-gel process and deposited by spin-coating technique. *Indian J. Pure Appl. Phys.* **2015**, *53*, 521–529.
4. Singh, A.K.; Singh, S.K. 7—Optical properties of ZnO. In *Nanostructured Zinc Oxide*; Elsevier: Amsterdam, The Netherlands, 2021; pp. 189–208. [[CrossRef](#)]
5. Mursal; Irhamni; Bukhari; Jalil, Z. Structural and Optical Properties of Zinc Oxide (ZnO) based Thin Films Deposited by Sol-Gel Spin Coating Method. *J. Phys. Conf. Ser.* **2018**, *1116*, 032020. [[CrossRef](#)]
6. Wisz, G.; Virt, I.; Sagan, P.; Potera, P.; Yavorskyi, R. Structural, Optical and Electrical Properties of Zinc Oxide Layers Produced by Pulsed Laser Deposition Method. *Nanoscale Res. Lett.* **2017**, *12*, 253. [[CrossRef](#)] [[PubMed](#)]
7. Kang, Y.; Yu, F.; Zhang, L.; Wang, W.; Chen, L.; Li, Y. Review of ZnO-based nanomaterials in gas sensors. *Solid State Ion.* **2021**, *360*, 115544. [[CrossRef](#)]
8. Dash, R.; Mahender, C.; Sahoo, P.K.; Soam, A. Preparation of ZnO layer for solar cell application. *Mater. Today Proc.* **2021**, *41*, 161–164. [[CrossRef](#)]
9. Galeazzi, R.; Panzo, I.J.; Becerril, T.; Morales, C.; Rosendo, E.; Silva, R.; Trujillo, R.; Coyopol, A.; Caballero, F.G.; Yarcé, L. Physicochemical conditions for ZnO films deposited by microwave chemical bath deposition. *RSC Adv.* **2018**, *8*, 8662–8670. [[CrossRef](#)]
10. Jangir, L.K.; Kumari, Y.; Kumari, P. 13—Zinc oxide-based light-emitting diodes and lasers. In *Nanostructured Zinc Oxide*; Elsevier: Amsterdam, The Netherlands, 2021; pp. 351–374. [[CrossRef](#)]
11. Jafarirad, S.; Salmasi, M.; Divband, B.; Sarabchi, M. Systematic study of Nd³⁺ on structural properties of ZnO nanocomposite for biomedical applications; in-vitro biocompatibility, bioactivity, photoluminescence and antioxidant properties. *J. Rare Earths* **2018**, *37*, 508–514. [[CrossRef](#)]
12. Gutiérrez, D.; Salgado, G.; Coyopol, A.; Rosendo, E.; Romano, R.; Morales, C.; Benítez, A.; Severiano, F.; Herrera, A.M.; González, F. Effect of the Deposit Temperature of ZnO Doped with Ni by HFCVD. *Materials* **2023**, *16*, 1526. [[CrossRef](#)] [[PubMed](#)]
13. Herrera, V.; Becerril, T.; Cervantes, E.; Salgado, G.; Galeazzi, R.; Morales, C.; Rosendo, E.; Coyopol, A.; Romano, R.; Caballero, F.G. Highly Visible Photoluminescence from Ta-Doped Structures of ZnO Films Grown by HFCVD. *Crystals* **2018**, *8*, 395. [[CrossRef](#)]
14. Rani, T.D.; Tamilarasan, K.; Elangovan, E.; Leela, S.; Ramamurthi, K.; Thangaraj, K.; Himcinschi, C.; Trenkmann, I.; Schulze, S.; Hietschold, M.; et al. Structural and optical studies on Nd doped ZnO thin films. *Superlattices Microstruct.* **2015**, *77*, 325–332. [[CrossRef](#)]

15. Poongodi, G.; Kumar, R.M.; Jayavel, R. Structural, optical and visible light photocatalytic properties of nanocrystalline Nd doped ZnO thin films prepared by spin coating method. *Ceram. Int.* **2015**, *41*, 4169–4175. [[CrossRef](#)]
16. Nistor, M.; Millon, E.; Cachoncinlle, C.; Ghica, C.; Hebert, C.; Perrière, J. Nd-doped ZnO films grown on c-cut sapphire by pulsed-electron beam deposition under oblique incidence. *Appl. Surf. Sci.* **2021**, *563*, 150287. [[CrossRef](#)]
17. Yatskiv, R.; Grym, J.; Bašínová, N.; Kučerová, Š.; Vaniš, J.; Piliai, L.; Vorokhta, M.; Veselý, J.; Maixner, J. Defect-mediated energy transfer in ZnO thin films doped with rare-earth ions. *J. Lumin.* **2023**, *253*, 119462. [[CrossRef](#)]
18. López, R.; Díaz, T.; García, G.; Galeazzi, R.; Rosendo, E.; Coyopol, A.; Pacio, M.; Juárez, H.; Oliva, A.I. Structural Properties of Zn-ZnO Core-Shell Microspheres Grown by Hot-Filament CVD Technique. *J. Nanomater.* **2012**, *2012*, 7. [[CrossRef](#)]
19. López, R.; Díaz, T.; Rosendo, E.; García, G.; Coyopol, A.; Juárez, H. Propiedades fotoluminiscentes de películas zno: A-SiO_x obtenidas por la técnica cvd asistido por filamento caliente. *Rev. Latinoam. Metal. Mater.* **2011**, *31*, 59–63.
20. López, R.; Díaz, T.; García, G.; Rosendo, E.; Galeazzi, R.; Juárez, H. Caracterización estructural y óptica de compósitos ZnO-SiO_x obtenidos por la técnica Cat-CVD. *Superf. Vacío* **2011**, *24*, 76–80.
21. López, R.; García, G.; Díaz, T.; Coyopol, A.; Rosendo, E.; Galeazzi, R.; Juárez, H.; Pacio, M. Low temperature growth of Zn-ZnO microspheres by atomic hydrogen assisted-HFCVD. *IOP Conf. Ser. Mater. Sci. Eng.* **2013**, *45*, 012016. [[CrossRef](#)]
22. López, R.; Díaz, T.; García, G.; Rosendo, E.; Galeazzi, R.; Coyopol, A.; Juárez, H.; Pacio, M.; Morales, F.; Oliva, A.I. Fast Formation of Surface Oxidized Zn Nanorods and Urchin-Like Microclusters. *Adv. Mater. Sci. Eng.* **2014**, *2014*, 4. [[CrossRef](#)]
23. López, R.; García, G.; Coyopol, A.; Díaz, T.; Rosendo, E. Effect of nitrogen gas in the agglomeration and photoluminescence of Zn-ZnO nanowires after high-temperature annealing. *Rev. Mex. Física* **2016**, *62*, 1–4.
24. Chauhan, S.; Kumar, M.; Chhoker, S.; Katyal, S. Structural, vibrational, optical and magnetic properties of sol-gel derived Nd doped ZnO nanoparticles. *J. Mater. Sci. Mater. Electron.* **2013**, *24*, 5102–5110. [[CrossRef](#)]
25. Mousavi, M.; Zinatloo, S.; Ghodrati, M. One-step sonochemical synthesis of Zn(OH)₂/ZnV₃O₈ nanostructures as a potent material in electrochemical hydrogen storage. *J. Mater. Sci. Mater. Electron.* **2020**, *31*, 17332–17338. [[CrossRef](#)]
26. Arunachalam, S.; Kirubasankar, B.; Murugadoss, V.; Vellamy, D.; Angaiyah, S. Facile synthesis of electrostatically anchored Nd(OH)₃ nanorods onto graphene nanosheets as high capacitance electrode material for supercapacitors. *New J. Chem.* **2018**, *42*, 2923–2932. [[CrossRef](#)]
27. Yuan, L.; Wang, C.; Cai, R.; Wang, Y.; Zhou, G. Temperature- dependent growth mechanism and microstructure of ZnO nanostructures grown from the thermal oxidation of zinc. *J. Cryst. Growth* **2014**, *390*, 101–108. [[CrossRef](#)]
28. Olvera, D.; Becerril, T.; Salgado, G.; Solís, A.; Andrés, E.; Isasmendi, R.; Sierra, R.; Ruiz, C.; Trujillo, R.; Caballero, F.G. Photoluminescent Enhancement by Effect of Incorporation Nickel in ZnO Films Grown. *Eur. J. Eng. Technol. Res.* **2021**, *6*, 177–180. [[CrossRef](#)]
29. Honglin, L.; Yingbo, L.; Jinzhu, L.; Ke, Y. Experimental and first-principles studies of structural and optical properties of rare earth (RE=La, Er, Nd) doped ZnO. *J. Alloys Compd.* **2014**, *617*, 102–107. [[CrossRef](#)]
30. Kumar, S.; Sahare, P.D. Nd-doped ZnO as a multifunctional nanomaterial. *J. Rare Earths* **2012**, *30*, 761. [[CrossRef](#)]
31. Jayachandriah, C.; Divya, A.; Kumar, K.; Krishnaiah, G. Effect of Nd on Structural and Optical Properties of Nd Doped ZnO Nanoparticles. In Proceedings of the International Conference on Advanced Nanomaterials & Emerging Engineering Technologies, Chennai, India, 24–26 July 2013.
32. Zhao, Z.; Song, J.; Zheng, J.; Lian, J. Optical properties and photocatalytic activity of Nd-doped ZnO powders. *Trans. Nonferrous Met. Soc. China* **2014**, *24*, 1434–1439. [[CrossRef](#)]
33. Wang, M.; Jiang, L.; Jung, E.; Hong, S. Electronic structure and optical properties of Zn(OH)₂: LDA+U calculations and intense yellow luminescence. *RSC Adv.* **2015**, *5*, 87496–87503. [[CrossRef](#)]

Disclaimer/Publisher's Note: The statements, opinions and data contained in all publications are solely those of the individual author(s) and contributor(s) and not of MDPI and/or the editor(s). MDPI and/or the editor(s) disclaim responsibility for any injury to people or property resulting from any ideas, methods, instructions or products referred to in the content.